

Master's Thesis

2013

First-principles thermodynamic study on the electrochemical stability of Pt nanoparticles in fuel cell applications

Joon Kyo Seo (2013.10.02 Birth)

Department of Energy Systems Engineering

2013

DGIST

2013

Master's Thesis

2013

First-principles thermodynamic study on the electrochemical stability of Pt nanoparticles in fuel cell applications

Joon Kyo Seo (2013.02.01 - 2013.02.01)

Department of Energy Systems Engineering

2013

DGIST

2013

First-principles thermodynamic study on the electrochemical stability of Pt nanoparticles in fuel cell applications

Advisor : Professor Byungchan Han

Co-advisor : Doctor Young-Gi Yoon

by

Joon Kyo Seo

Department of Energy Systems Engineering

DGIST

A thesis submitted to the faculty of DGIST in partial fulfillment of the requirements for the degree of Master of Science in the Department of Energy Systems Engineering. The study was conducted in accordance with Code of Research Ethics¹.

12. 5. 2012

Approved by

Professor Byungchan Han _____

(Advisor)

Doctor Young-Gi Yoon _____

(Co-Advisor)

¹ Declaration of Ethical Conduct in Research: I, as a graduate student of DGIST, hereby declare that I have not committed any acts that may damage the credibility of my research. These include, but are not limited to: falsification, thesis written by someone else, distortion of research findings or plagiarism. I affirm that my thesis contains honest conclusions based on my own careful research under the guidance of my thesis advisor.

First-principles thermodynamic study on the electrochemical stability of Pt nanoparticles in fuel cell applications

Joon Kyo Seo

Accepted in partial fulfillment of the requirements for the degree of
Master of Science.

12. 5. 2012

Head of Committee Byungchan Han (±-)

Prof. >ä&Y5´

Committee Member Young-Gi Yoon (±-)

Dr. 0~1/‰o ,

Committee Member Hasuck Kim (±-)

Prof. È>à*¥

MS/ES
201124009

서준교. Joonkyo Seo. First-principles thermodynamic study on the electrochemical stability of Pt nanoparticles in fuel cell applications. Department of Energy Systems Engineering. 2013. 25P. Advisor Prof. Byungchan Han, Co-Advisor Dr. Young-Gi Yoon.

Abstract

Durability of Pt based nanocatalyst materials in acidic environments is one of the key issues hindering the development of efficient fuel cells. In this study, we used first principles calculations to analyze the electrochemical degradation of Pt nanoparticles. Model systems for Pt nanoparticles of different sizes were conceptualized for calculating their electrochemical dissolution potential, which essentially indicates the thermodynamic driving force for the dissolution. The dissolution mechanism for Pt atoms on the outermost shell of the nanoparticle by accounting for various possible pathways which lead to complete dissolution. Based strictly on thermodynamic considerations, our findings point towards a strong size dependent behavior of the Pt nanoparticles, whose properties become similar to bulk Pt for size more than 3 nm. Remarkably, we find that for all cases, the dissolution proceeds by exposing more (111) facets at the expense of other atomic sites. Our results indicate that the competition between two major thermodynamic factors, the cohesive energy and the surface energy, decides the dissolution pathway. Based on our findings, we propose some desired characteristics which can serve towards rational design of model Pt nanocatalysts. Our findings may be of importance in understanding of the electrochemical stability in other applications as well, for instance the photo-catalysts for fuel generations via water splitting.

Keywords: Density functional theory, Fuel cell, Nanocatalyst, Stability, Degradation mechanism

Contents

Abstract	1
List of contents	2
List of figures	3
Chapter 1. Introduction	4
1.1 Challenges of fuel cells	4
1.2 Objectives of this work	9
Chapter 2. Methodology	4
2.1 Model systems	4
2.2 Computational details	7
2.3 Formalisms	8
Chapter 3. Results and discussion	10
Chapter 4. Limitations of the thesis and future works	17
Chapter 5. Conclusions	19
References	21
Summary (Appendix)	25

Acknowledgments (Appendix)

Curriculum Vitae

List of figures

Figure 1. Model systems of Pt nanoclusters (1.1, 1.6, 2.2 and 2.7 nm in diameters) Symmetrically inequivalent atomic sites on the outermost shells are marked by circles according to their local environments.

Figure 2. Dissolution candidates of outermost shell (Diameter of model system: 2.2 nm).

Figure 3. The electrochemical dissolution of nanoparticle (diameter of model systems: 2.7, 2.1, 1.6 and 1.1 nm). Δ represents ab-initio calculated dissolution potential of dissolution candidates for each nanoparticle (upper illustration). Red solid line indicates the lowest dissolution potential when particular atoms (yellow color of lower illustration) are dissolving.

Figure 4. Cohesive energy for nanoparticle as a function of the number of atoms. Triangular represents ab-initio calculated cohesive energy per atom in which blue triangle is the model system and red one is the intermediate structure appeared by the viable dissolution path. Red line denotes the upper bound the calculated cohesive energies of intermediate structures.

Chapter 1

Introduction

1.1 Challenges of fuel cells

Proton Exchange Membrane (PEM) fuel cells are one of the key technologies for harvesting clean and environmentally friendly energy sources ¹. Since first serving as the power source of the Gemini space shuttle in 1960s, fuel cells have been extensively studied to replace conventional fossil fuels for transportation vehicles. However, several long standing issues such as high catalyst cost and low oxygen reduction reaction (ORR) efficiency of Pt catalysts have been a hindrance to its widespread commercialization. Experimental and computational studies over the last few decades have been focused on the utilization of nanoscale Pt particles as novel functional catalysts mainly because of their high surface to volume ratio ²⁻⁴. Indeed, several pure or Pt based alloy nanoparticles have been identified as materials showing substantially improved catalytic activities ^{5,6}.

According to recent reports, however, it has been observed that the structural integrity of Pt nanoparticles can be seriously degraded in acidic media, which diminishes the durability to a non-acceptable level of fuel cell performance ⁷⁻⁹. Several mechanisms underlying the degradation phenomena have been proposed: pseudo-Ostwald ripening (dissolution of catalysts into electrolyte and

re-deposition into larger a particle)⁷, direct electrochemical dissolution of metal into acidic electrolyte¹⁰, and corrosion of support materials¹¹, and others. Depending on the operational conditions of fuel cells and topologies of catalyst layers, each or several of these mechanisms may combine in a parallel way and drive such catalytic degradation¹².

Especially, the direct electrochemical dissolution is interesting because in its bulk form, Pt is chemically the noblest metal. Nevertheless, an agreement on the detailed dissolution process at the atomic scale is largely missing. For example, experimental observations combined with density functional theory (DFT) calculations have shown that Pt nanoparticles smaller than 2 nm exposed to acidic media disappear from Au support in a short time scale¹⁰, while other reports propose that the Pt^{2+} ions in acidic electrolyte mainly come from a stepwise atomic dissolution on the outermost shell¹³.

1.2 Objectives of this work

An accurate understanding of the electrochemical degradation process at atomic level is an important step towards achieving the development of functional catalysts of not only high durability but also high efficiency. In this paper we extensively utilized first principles DFT calculations to cap-

ture the atomic level pictures showing thermodynamically the most plausible dissolution path as a function of Pt nanoparticle size. Ab-initio thermodynamics allow us to optimize Pt nanostructure, enabling the capture of the evolution of nanoparticle morphologies as the electrochemical dissolution proceeds. Our results clearly show that a subtle interplay between the surface energy and the cohesive energy control catalytic degradation of Pt nanoparticle.

Chapter 2

Methodology

2.1 Model systems

We setup a model system to simulate Pt nanoparticles as a function of size: Pt_{55} (55 atoms of 1.1 nm), Pt_{147} (147 atoms of 1.6 nm), Pt_{309} (309 atoms of 2.2 nm) and Pt_{561} (561 atoms of 2.7 nm) as shown in Fig. 1. We defined the size of a nanoparticle as the distance between two diametrically opposite vertex sites. We adopted the typically regarded nanocatalysts in fuel cell applications

14-17.

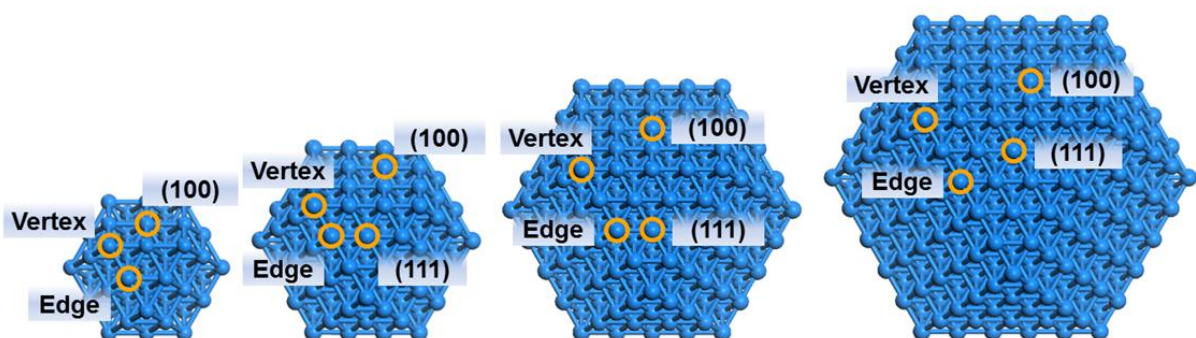


Fig. 1. Model systems of Pt nanoclusters (1.1, 1.6, 2.2 and 2.7 nm in diameters). Symmetrically inequivalent atomic sites on the outermost shells are marked by circles according to their local environments

Since dissolution potential of an individual atom in the Pt nanoparticles may depend on its local environment (i.e., the coordination number and geometry) we identified four types of symmetrically inequivalent atomic sites on the outermost shell, namely: vertex, edge, (100) and (111) facets as shown in Fig. 1. Each of these sites were then grouped together with their same kind resulting in four basic candidates with atomic sites that could be subjected to simultaneous dissolution owing to their nearly symmetric location on the surface of the nanoparticle, as shown in Fig. 2(a-d). It should be noted that because the dissolution process is assumed to take place simultaneously at all candidate sites in a symmetric manner, we ignore the minor local asymmetry within the edge sites and (100) facets. Also, further combinations of these four basic candidates result in other candidates with atomic sites that could be subjected to simultaneous dissolution as shown in Fig. 2(e-o).

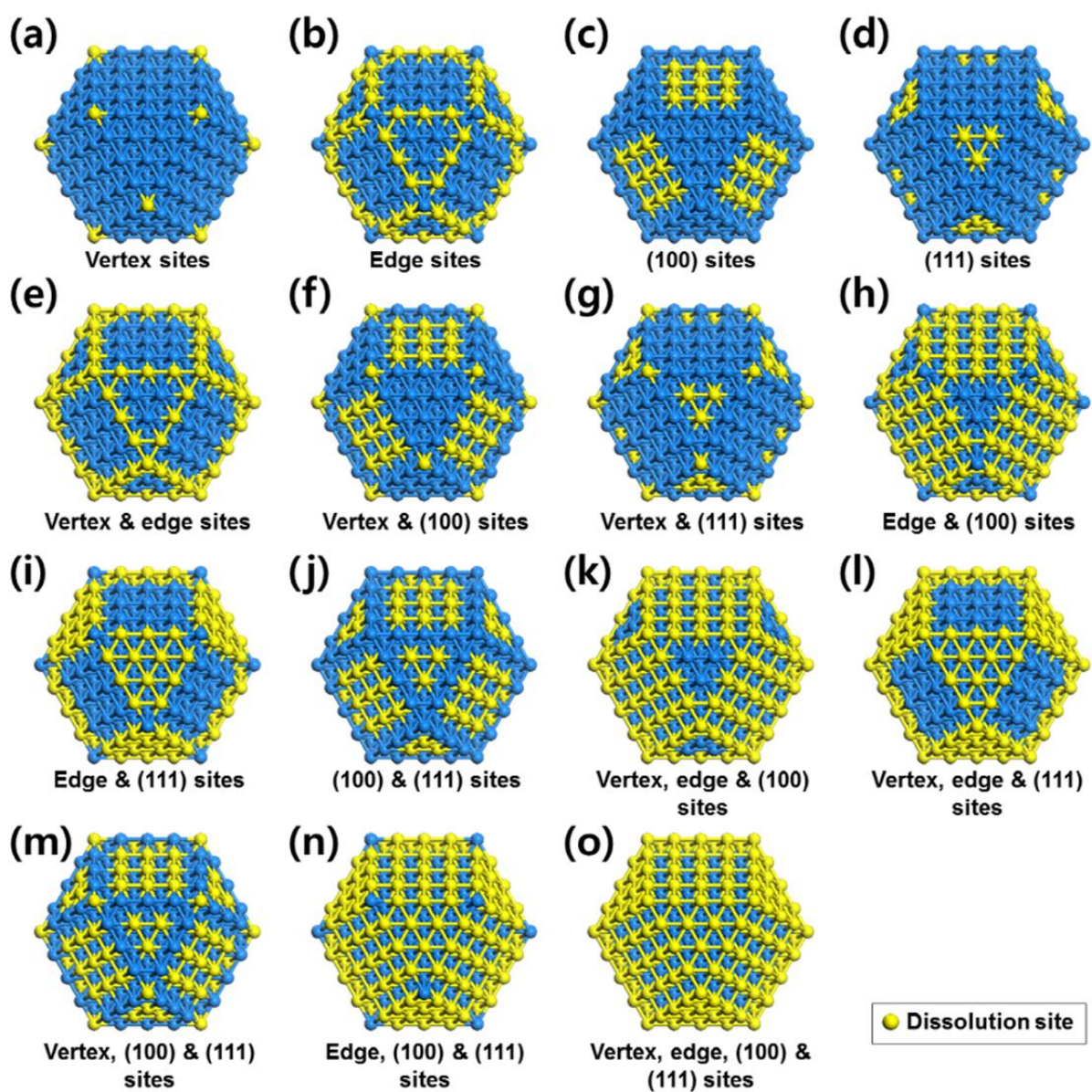


Fig. 2. Dissolution candidates of outermost shell (Diameter of model system: 2.2 nm).

Using first principles, we calculated the dissolution potentials for each of the candidates corresponding to the model system for its first dissolution step in which all the yellow atoms, as shown in Fig. 2, were removed simultaneously. As the dissolution potential is a measure of resistance against

electrochemical degradation, we chose the viable path of dissolution mechanism to be occurring through the candidate which had the lowest evaluated dissolution potential at each step. After completion of the first dissolution step, the resultant structure was then selected as the initial model system for the next dissolution step, and we again identified possible dissolution candidates for this new model system using the same procedure as described above. This process was repeated until a single atom remained, thus unveiling the most thermodynamically viable pathway to complete dissolution of the nanoparticle.

2.2 Computational details

We used the generalized gradient approximation (GGA) ¹⁸ by Perdew, Burke and Ernzerhof (PBE) ¹⁹ implemented in Vienna Ab-initio Simulation Package (VASP) ¹⁸ to describe exchange-correlation energies among electrons. Pseudo-potentials generated by projector augmented wave (PAW) method ^{20,21} were used to replace interaction potentials of core electrons. A gamma point mesh with 1 x 1 x 1 *k*-point was used. We imposed a periodic boundary condition on our model systems with vacuum space as thick as the twice of the cluster size to prohibit interactions among the images. All atoms are fully relaxed to calculate the optimized structures of each the Pt model nano-

particle with a cutoff energy of 325 eV for plane wave basis set. The lattice constant of a bulk fcc Pt

PHWDO ZDV FDOFXODWHG LQ WKLV VWXGHQW. Experimental measurements of the

XHRI²². ‡

2.3 Formalisms

It has been proposed¹⁰ that Pt nanoparticles degrade electrochemically by direct dissolution of surface atoms into acidic media as shown in eq.(1).



Where Pt_n and Pt_{n-m} are the nanoparticles consisting of n and $n-m$ Pt atoms respectively.

Eq.(1) describes a reversible reaction where m atoms on the outermost shell of the Pt nanoparticle are ionized to Pt^{2+} , and its dissolution potential is calculated as given in eq.(2) in reference to the Standard Hydrogen Electrode (SHE).

$$U_m = \frac{1}{2me} \{E(Pt_{n-m}) - E(Pt_n)\} + \frac{1}{2e} \{ \mu^\circ(Pt^{2+}, aq) + kT \log_e(a_{Pt^{2+}}) \} \quad (2)$$

Where, E indicates ab-initio DFT calculated total energy, and μ° , k , T , $a_{Pt^{2+}}$ have their usual meanings: chemical potential of Pt^{2+} ions at standard conditions, Boltzmann constant, absolute temperature, and activity of Pt^{2+} ions respectively. Instead of calculating the ionic solvation ener-

gy of Pt^{2+} ions ($\mu^o(Pt^{2+}, aq)$) with ab-initio DFT methods, which is in fact not easy ²³, we utilized

the electrochemical dissolution reaction of bulk Pt as shown in eq.(3)



The dissolution potential of a bulk Pt in eq.(3) is given by eq.(4) as

$$U_{bulk} = \frac{1}{2e} \{ \mu^o(Pt^{2+}, aq) + kT \log_e(a_{Pt^{2+}}) - E(Pt_{bulk}) \} \quad (4)$$

Where U_{bulk} is known as 1.011 V (SHE) ²⁴ under assumption that the concentration of $[Pt^{2+}]$ is

equal to 10^{-6} M ¹⁰. Our DFT calculations showed that the energy per atom of bulk Pt ($E(Pt_{bulk})$)

is -6.03 eV. Using eq.(2) and eq.(4), U_m is expressed in eq.(5) as

$$U_m = U_{bulk} + \frac{1}{2me} \{ E(Pt_{n-m}) + mE(Pt_{bulk}) - E(Pt_n) \} \quad (5)$$

We ab-initio calculated U_m for each of the dissolution candidates of the model systems and those

of subsequently appearing structures which are encountered during the most thermodynamically

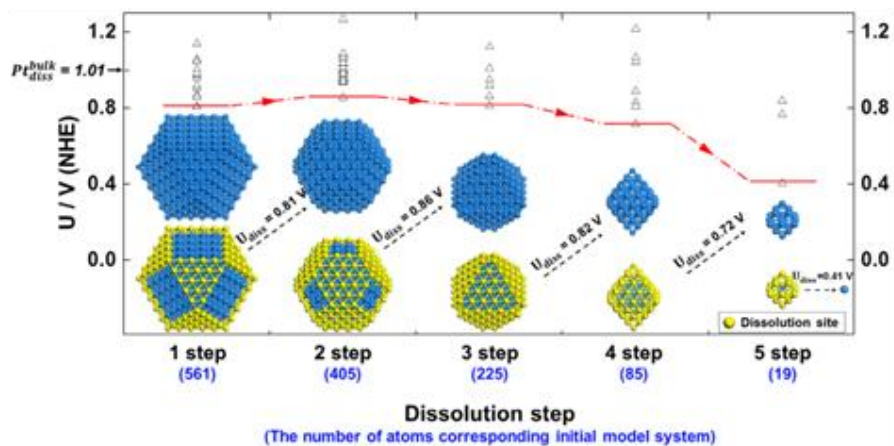
viable dissolution path.

Chapter 3

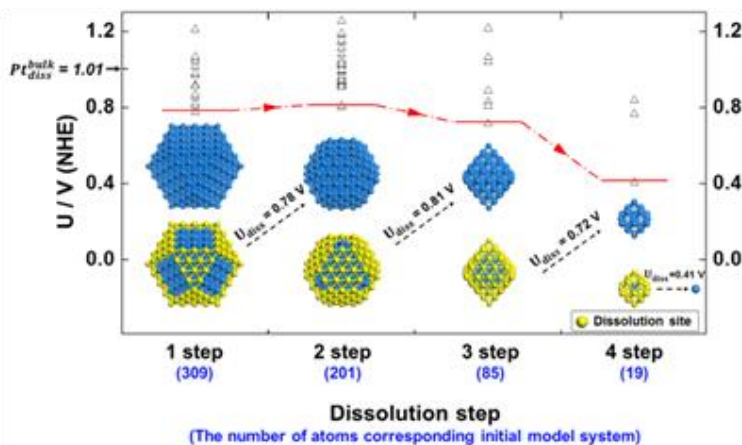
Results and discussion

We calculated the dissolution potentials by applying the formalism as described earlier to the four model systems. Fig. 3 shows the ab-initio calculated dissolution potentials U_m of Pt nanoparticles as a function of their size. For example, Fig. 3(a) shows the dissolution pathway for the Pt nanoparticle of size 2.7 nm which is composed of 561 atoms. For each dissolution step, several dissolution candidates were systematically considered for evaluation of their dissolution potentials. The calculated dissolution potentials were plotted corresponding to the size of the initial model system for that step. The candidate with the lowest dissolution potential was selected for simultaneous removal of the atomic sites which are marked in yellow atom. The nanocluster thus obtained served as the initial model system for the next dissolution step.

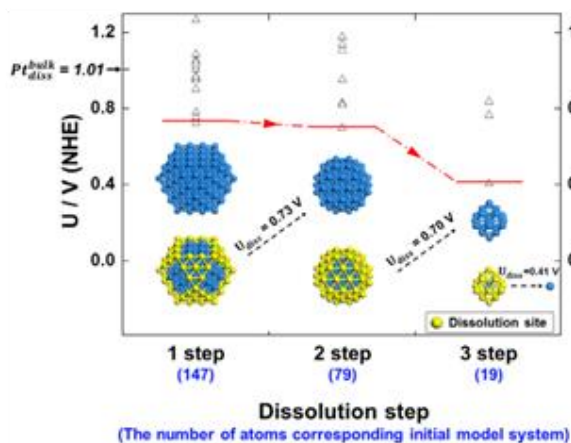
(a) Pt_{561} ($d = 2.7$ nm)



(b) Pt_{309} ($d = 2.2$ nm)



(c) Pt_{147} ($d = 1.6$ nm)



(d) Pt_{55} ($d = 1.1$ nm)

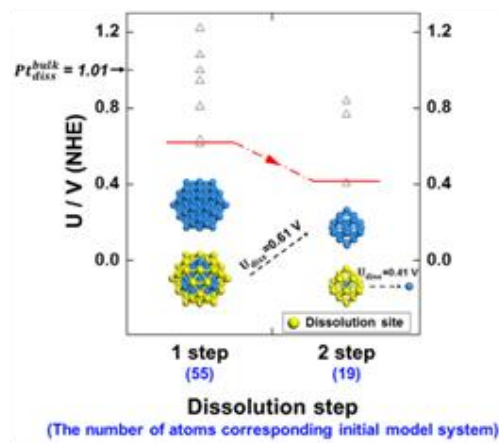


Fig. 3. The electrochemical dissolution of nanoparticle (diameter of model systems: 2.7, 2.1, 1.6 and 1.1 nm). \triangle represents ab-initio calculated dissolution potential of dissolution candidates for each nanoparticle (upper illustration). Red solid line indicates the lowest dissolution potential when particular atoms (yellow color of lower illustration) are dissolving.

The numbers at each step in Fig. 3(a) represent the number of atoms for the nanoparticle that served as the initial model system for that dissolution step. The procedure was followed until a single atom remained. The red line, which is constructed by joining the points corresponding to the lowest dissolution potentials, denotes the most thermodynamically viable path for step-by-step dissolution. A similar methodology was employed for constructing the plots for other model systems. Our results indicate that Pt nanoclusters of size smaller than about 3 nm have weaker electrochemical stability than bulk Pt (1.01 V vs. SHE), which is in agreement with previous reports ¹⁰.

On observing closely, we find that at each dissolution step, the dissolution proceeds in a manner such that the structures emerging after dissolution reveal a larger fraction of atoms on the outermost shell that belong to the (111) facets, at the expense of the atoms located at edges, vertices, and (111) facets. For example, for the Pt nanocluster composed of 561 atoms (about 2.7 nm), the 1st dissolution step results in an increased fraction of the surface area covered by the (111) planes by removing the atoms marked in yellow, thus leading to a truncated-octahedron structure composed of 405 atoms. It is not surprising that this characteristic of the dissolution mechanism is evident across all model systems, as the presence of a larger fraction of (111) facet leads to a relatively more stabilized nanoparticle. The (111) facet is rigorously known to be the most stable of all

extended Pt surfaces with the lowest surface energy ²⁵.

Remarkably, for model systems Pt_{561} (Fig. 3a) and Pt_{309} (Fig. 3b), the dissolution potential along the thermodynamically most viable path (red line) at the second step increases to a value slightly greater than what is observed at the first step. This is an indication that the nanoparticle obtained after the first step for these two cases is more durable than the model system itself, possibly owing to an increase in the fraction of the stabilizing (111) facet. However, these values subsequently decrease rapidly as the nanoparticle size decreases. Thus, one finds that the thermodynamics of the dissolution mechanism is probably also influenced by the size of the nanoparticle, apart from the surface energy, as has been observed in this study.

We propose that at least two thermodynamic factors control the electrochemical dissolution process. We believe that it is a subtle interplay between the size dependent cohesive energy (per atom) and the surface energy in energetically stabilizing the Pt nanocluster. In each dissolution step the surface energy gets minimized as much as other constraints, such as the strain on the shell allow, while simultaneously, the cohesive energy (per atom) is lowered due to the decreasing size of the nanoparticle. While lower surface energies add to the stability, lower cohesive energies (per atom) decrease the stability of the nanoparticle. Indeed, it has been already proposed that weak co-

hesive energy is a major driving force behind the electrochemical degradation of Pt nanoparticles via dissolution into acidic solution^{10,26}. However, a detailed study and analysis of how the structures evolve with the electrochemical dissolution steps has not been performed yet.

To understand the evolution of nanoparticle structures to a greater detail, we calculated cohesive energies of Pt nanoparticles as a function of size (or the number of total atoms in the cluster, N) from first principles and plotted them, as shown in Fig. 4. It can be seen that the cohesive energy per atom decreases dramatically as size decreases below about 250 atoms. For nanoclusters larger than about 250 atoms in size, a slowly decaying behavior of cohesive energy can be observed with decreasing size. In this region, the stabilizing effect of the increasing (111) surface area fraction is dominant. This interplay very much explains the slight increase in dissolution potentials after the first step in model systems Pt_{561} and Pt_{309} . For the nanoparticle of size smaller than this, the stabilizing effect of increased (111) surface fraction is overpowered by the destabilizing effect of cohesive energy. Hence, the dissolution potential for such nanoparticles decreases with their size. We propose that it is the size dependent competition between these two factors that dictates the most thermodynamically viable mechanism. The influence of these factors is well reflected in our calculated results.

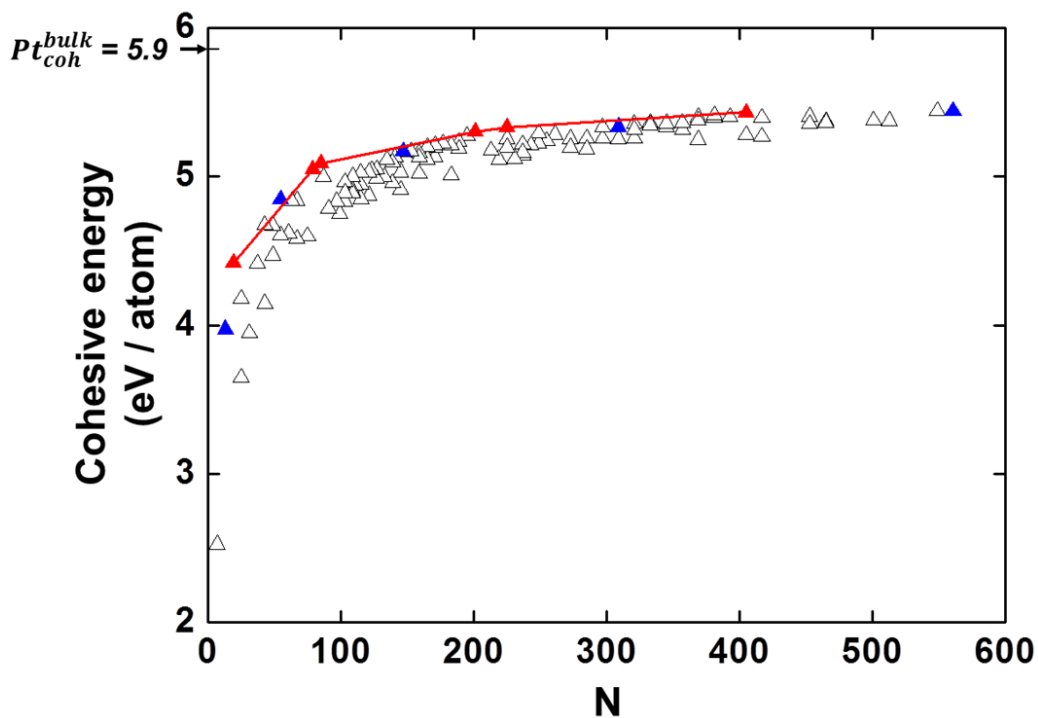


Fig. 4. Cohesive energy for nanoparticle as a function of the number of atoms. Triangular represents ab-initio calculated cohesive energy per atom in which blue triangle is the model system and red one is the intermediate structure appeared by the viable dissolution path. Red line denotes the upper bound the calculated cohesive energies of intermediate structures.

Furthermore, the thermodynamic dissolution path identified here agrees well with the red line denoting the reverse cohesive energy convex hull, as shown in Fig. 4. This observation is succinctly represented by the red triangles on this line, which correspond to the intermediate structures that were encountered on the most thermodynamically viable dissolution paths across all model systems. The red line marks the upper bound of the calculated cohesive energies and indicates the most stable scenarios for a given particle size. Thus we assert that our proposed dissolution pathways, which are based on only thermodynamic considerations, are strongly founded. Remarkably,

we also find that the nanoclusters corresponding to these red triangles are quite similar to the close-ordered Pt nanoclusters, which have also been found to be relatively stable ^{14,15}.

Our results create the groundwork for conceptually designing highly durable Pt catalysts with minimal material cost, which may be achieved using novel methodologies that expose more (111) planes on the outermost shell ^{27,28}, keeping in mind that the particle size should be at least larger than 3 nm. It has been previously reported that, the (100) Pt facets contribute to ORR activity much less than (111) Pt facets ²⁹. We believe that designing Pt nanoparticles with high area fraction of (111) planes and minimal (100) planes to accommodate the strain field may be a rational way to satisfy the ORR activity and electrochemical durability issues. It is worth mentioning that recent reviews on the current state of conceptual catalyst designing have pointed out that Pt₃Ni nanoparticles produced with predominantly (111) facets have shown up to 4 fold mass activity compared to the most commonly and commercially available Pt/C nanocatalysts ³⁰. Another study on the nano-size effect of Pt monolayer catalyst nanoparticles synthesized with Pd and Pd₃Co cores reported 2 to 3 fold enhancement in specific activity owing to the lattice mismatch and contraction effects on the (111) Pt facets ³¹.

Chapter 4

Limitations of the thesis and future works

In the present work, we studied the ab-initio thermodynamic aspects to identify the most viable electrochemical dissolution path. This implies that our arguments will be fully ensured on the condition that thermodynamic driving force is enough to get over any kinetic activation processes, if there are any. For example, at each dissolution step the Pt atoms should be mobile to achieve reconstruction into the thermodynamically most stable configuration. Besides, we did not consider other possible mechanisms of catalyst degradation such as pseudo-Ostwald ripening, support corrosion, Pt dissolution into electrolyte and re-deposition into a larger particle, etc. As the particle size decreases, Pt nanoclusters can coagulate into bigger particles instead of structural optimization of a single Pt cluster to minimize surface energy.

In addition, our model systems do not incorporate the effect of supports. Recently it has been reported that several carbon-based novel structures³²⁻³⁶ and ceramic materials have shown³⁷⁻⁴¹ their distinctive stability compared to conventional carbon supports that they might enhance the stability of nanocatalysts too. There are several novel substrates that we can take into account. First, a study on the nitrogen containing carbon nanotube revealed the tubular morphology and the nitrogen

functionality of the support have influence on the stability of the electrode ³⁴. In addition, the boron-doped diamonds possesses properties that ideally suited for morphological stability and corrosion resistance compared to carbon support materials ^{35,36}. Likewise, ceramic materials such as titanium based oxides ^{37,40,41} are also interesting catalyst supports to be investigated with ab-initio DFT calculations.

We expect that the dissolution characteristics found in this thesis are very useful to understand the stability of nanocatalysts on those durable supports so that it can give insight on developing high-performance fuel cells.

Chapter 5

Conclusions

In this study, we analyzed the degradation phenomena of Pt nanoclusters in acidic environment by looking specifically the electrochemical degradation mechanism. We set up model systems of four different sizes, each having the shape of cubo-octahedron. Further, we identified various candidates for step by step electrochemical dissolution, under the assumption of simultaneous dissolution of Pt atoms from the outermost shell. The dissolution mechanism was allowed to proceed thermodynamically, only via the candidate with the lowest calculated value of the dissolution potential, which was evaluated using first principles density functional theory.

Our results lead us to some remarkable observations. The mechanism proceeds at each step by exposing more of the (111) facets at the expense of other sites on the outermost shell of the Pt nanocluster, which is widely known to be the most stable of all extended Pt surfaces. We found a strong size dependent behavior of the dissolution potential, especially for smaller sized nanoparticles which can be attributed to the strong decay of cohesive energy with decreasing size. Based on the particular trends in the values of dissolution potentials that emerge during the step by step process, we argued that the overall mechanism is dictated by the competition between the stabilizing

effect of the increasing (111) surface area fraction on the outer most shell and the destabilizing effect due to decreasing cohesive energy, as the dissolution proceeds. We also found that the intermediate structures, which were encountered across all model systems, lie on the upper bound of the cohesive energy values corresponding to a given nanoparticle size, indicating them to be stable nanoparticles. These findings create a very strong case for the thermodynamically driven mechanism proposed in this study. Furthermore, these structures were found to be quite similar to the magic numbered clusters known for their relatively high stability.

References

- 1 Carrette, L., Friedrich, K. A. & Stimming, U. Fuel Cells: Principles, Types, Fuels, and Applications. *ChemPhysChem* **1**, 162 (2000).
- 2 Greeley, J., Stephens, I. E. L., Bondarenko, A. S., Johansson, T. P., Hansen, H. A., Jaramillo, T. F., Ros VP HLVO - & KR UNHQGRUII , 1°UVNRY - . \$OOR\ V RI S metals as oxygen reduction electrocatalysts. *Nat. Chem.* **1**, 552 (2009).
- 3 Gasteiger, H. A. & Markovic, N. M. Just a Dream § or Future Reality? *Science* **324**, 48 (2009).
- 4 Stamenkovic, V. R., Fowler, B., Mun, B. S., Wang, G., Ross, P. N., Lucas, C. A. & Markovic, N. M. Improved Oxygen Reduction Activity on Pt₃Ni(111) via Increased Surface Site Availability. *Science* **315**, 493 (2007).
- 5 Strasser, P., Koh, S., Anniyev, T., Greeley, J., More, K., Yu, C., Liu, Z., Kaya, S., Nordlund, D., Ogasawara, H., Toney, M. F. & Nilsson, A. Lattice-strain control of the activity in dealloyed core-shell fuel cell catalysts. *Nat. Chem.* **2**, 454 (2010).
- 6 Kuttiyiel, K. A., Sasaki, K., Choi, Y., Su, D., Liu, P. & Adzic, R. R. Bimetallic IrNi core platinum monolayer shell electrocatalysts for the oxygen reduction reaction. *Energy Environ. Sci.* **5**, 5297 (2012).
- 7) H U U H L U D 3 - 2 + Horn, Y., Morgan, D., Markharia, R., Kocha, S. & Gasteiger, H. A. Instability of Pt/C Electrocatalysts in Proton Exchange Membrane Fuel Cells. *J. Electrochem. Soc.* **152**, A2256 (2005).
- 8 Shao-Horn, Y., Sheng, W. C., Chen, S., Ferreira, P. J., Holby, E. F. & Morgan, D. Instability of Supported Platinum Nanoparticles in Low-Temperature Fuel Cells. *Top. Catal.* **46**, 285 (2007).
- 9 Holby, E. F., Sheng, W., Shao-Horn, Y. & Morgan, D. Pt nanoparticle stability in PEM fuel cells: influence of particle size distribution and crossover hydrogen. *Energy Environ. Sci.* **2**, 865 (2009).
- 10 Tang, L., Han, B., Persson, K., Friesen, C., He, T., Sieradzki, K. & Ceder, G. Electrochemical Stability of Nanometer-Scale Pt Particles in Acidic Environments. *J. Am. Chem. Soc.* **132**, 596 (2010).
- 11 Maass, S., Finsterwalder, F., Frank, G., Hartmann, R. & Merten, C. Carbon support oxidation in PEM fuel cell cathodes. *J. Power Sources* **176**, 444 (2008).
- 12 Meier, J. C., Katsounaros, I., Galeano, C., Bongard, H. J., Topalov, A. A., Kostka, A.,

- Karschin, A., Schuth, F. & Mayrhofer, K. J. J. Stability investigations of electrocatalysts on the nanoscale. *Energy Environ. Sci.* **5**, 9319 (2012).
- 13 Komanicky, V., Chang, K. C., Menzel, A., Markovic, N. M., You, H., Wang, X. & Myers, D. Stability and Dissolution of Platinum Surfaces in Perchloric Acid. *J. Electrochem. Soc.* **153**, B446 (2006).
- 14 Tao, A. R., Habas, S. & Yang, P. Shape Control of Colloidal Metal Nanocrystals. *Small* **4**, 310 (2008).
- 15 Klabunde, K. J. & Richards, R. M., Nanoscale Materials in Chemistry, 2nd ed., *John Wiley & Sons*, Hoboken, 27, (2009).
- 16 Mayrhofer, K. J. J., Blizanac, B. B., Arenz, M., Stamenkovic, V. R., Ross, P. N. & Markovic, N. M. The Impact of Geometric and Surface Electronic Properties of Pt-Catalysts on the Particle Size Effect in Electrocatalysis. *J. Phys. Chem. B* **109**, 14433 (2005).
- 17 Kinoshita, K. Particle Size Effects for Oxygen Reduction on Highly Dispersed Platinum in Acid Electrolytes. *J. Electrochem. Soc.* **137**, 845 (1990).
- 18 Perdew, J. P., Burke, K. & Ernzerhof, M. Generalized Gradient Approximation Made Simple. *Phys. Rev. Lett.* **77**, 3865 (1996).
- 19 Blochl, P. E. Projector augmented-wave method. *Phys. Rev. B* **50**, 17953 (1994).
- 20 Kresse, G. & Joubert, D. From ultrasoft pseudopotentials to the projector augmented-wave method. *Phys. Rev. B* **59**, 1758 (1999).
- 21 Kittel, C., Introduction to Solid State Physics, 8th ed., *Wiley*, New York, 20, (2004).
- 22 Tomasi, J., Mennucci, B. & Cammi, R. Quantum Mechanical Continuum Solvation Models. *Chem. Rev.* **105**, 2999 (2005).
- 23 Pourbaix, M., Atlas of Electrochemical Equilibria in Aqueous Solutions, 2nd ed., *National Association of Corrosion Engineers*, Houston, 378, (1974).
- 24 Vitos, L., Ruban, A. V., Skriver, H. L. & Kollar, J. The surface energy of metals. *Surf. Sci.* **411**, 186 (1998).
- 25 Qi, W. H. & Wang, M. P. Size effect on the cohesive energy of nanoparticle. *J. Mater. Sci. Lett.* **21**, 1743 (2002).
- 27 Wu, J., Zhang, J., Peng, Z., Yang, S., Wagner, F. T. & Yang, H. Truncated Octahedral Pt₃Ni Oxygen Reduction Reaction Electrocatalysts. *J. Am. Chem. Soc.* **132**, 4984 (2010).

- 28 Zhang, J., Yang, H., Fang, J. & Zou, S. Synthesis and Oxygen Reduction Activity of Shape-Controlled Pt₃Ni Nanopolyhedra. *Nano Lett.* **10**, 638 (2010).
- 29 Han, B., Viswanathan, V. & Pitsch, H. First-Principles Based Analysis of the Electrocatalytic Activity of the Unreconstructed Pt(100) Surface for Oxygen Reduction Reaction. *J. Phys. Chem. C* **116**, 6174 (2012).
- 30 Debe, M. K. Electrocatalyst approaches and challenges for automotive fuel cells. *Nature* **486**, 43 (2012).
- 31 Wang, J. X., Inada, H., Wu, L., Zhu, Y., Choi, Y., Liu, P., Zhou, W.-P. & Adzic, R. R. Oxygen Reduction on Well-Ordered Pt Nanocatalysts: Particle Size, Facet, and Pt Shell Thickness Effects. *J. Am. Chem. Soc.* **131**, 17298 (2009).
- 32 Stevens, D., Hicks, M., Haugen, G. & Dahn, J. Ex Situ and In Situ Stability Studies of PEMFC Catalysts Effect of Carbon Type and Humidification on Degradation of the Carbon. *J. Electrochem. Soc.* **152**, A2309-A2315 (2005).
- 33 Guo, D. J. & Li, H. L. Electrocatalytic oxidation of methanol on Pt modified single-walled carbon nanotubes. *J. Power Sources* **160**, 44-49 (2006).
- 34 Maiyalagan, T., Viswanathan, B. & Varadaraju, U. Nitrogen containing carbon nanotubes as supports for Pt alternate anodes for fuel cell applications. *Electrochem. Commun.* **7**, 905-912 (2005).
- 35 Chen, Q., Granger, M. C., Lister, T. E. & Swain, G. M. Morphological and Microstructural Anodic Current Densities. *J. Electrochem. Soc.* **144**, 3806-3812 (1997).
- 36 Hupert, M., Muck, A., Wang, J., Stotter, J., Cvackova, Z., Haymond, S., Show, Y. & Swain, G. M. Conductive diamond thin-films in electrochemistry. *Diam. Relat. Mater.* **12**, 1940-1949 (2003).
- 37 Huang, S.-Y., Ganesan, P., Park, S. & Popov, B. N. Development of a Titanium Dioxide-Supported Platinum Catalyst with Ultrahigh Stability for Polymer Electrolyte Membrane Fuel Cell Applications. *J. Am. Chem. Soc.* **131**, 13898 (2009).
- 38 Bavykin, D. V., Friedrich, J. M. & Walsh, F. C. Protonated titanates and TiO₂ nanostructured materials: synthesis, properties, and applications. *Adv. Mater.* **18**, 2807-2824 (2006).
- 39 Raghuvver, V. & Viswanathan, B. Synthesis, characterization and electrochemical studies of Ti-incorporated tungsten trioxides as platinum support for methanol oxidation. *J. Power Sources* **144**, 1-10 (2005).

- 40 Diebold, U. The surface science of titanium dioxide. *Surf. Sci. Rep.* **48**, 53-229 (2003).
- 41 Fovet, Y., Gal, J. Y. & Toumelin-Chemla, F. Influence of pH and fluoride concentration on titanium passivating layer: stability of titanium dioxide. *Talanta* **53**, 1053-1063 (2001).

õ\$À0 /

1#1 0X#410E*80Û01>ä/x"T10E3H0!%1• 6'#10à 10E ,?Ü>á1%o

.Ð1•*1/X ^>ä //u>á1%o ' *¥

*8*1?à E/X*# %1• 1 1 0à //?Ü \$À1# h*1- /x"T10E3H# #%#>ð/X 1 /<*#
^1- >ý,tü ' ' 0ü l . &€ \$À/X*# //u>á1%o ^1~0ì ,% 0Ä!ä >à/t %1• 1 1 0à
10E ,?Ü>á1%||?Ü?0E*10ì d\$ >à , 00E>ü 1#1 0X#410E*80ì L1 >à/^ l . //?Ü?0E*10È 10E ,?Ü>á1%
01>ü10E00E/È!°0ü 1 ø 0ü# L*8>à , 00E>ü3 nm 0ü>à %1• 1 1 \$0 0ì *À0h l . €#4 h
0ü 0ü /ì10E01>ü/X 0ü"ü /t!t "p<@# *- \$ >à , 00E>ü 1 1 0à 6ä0 ... U3P0ü p L1%0Ä!ä
01>ü /< *# /N/<3H + 00E TStep by step TT #Ü8l P3 0ì L1 >à/^ l . € 8,, , %1•
1 1 0à 01>ü10E00E ^1 1 9ô ,/X 0à>ü 2 08 h , 9ô , ^ 8l3P+!ä & 9ô %1• •+ 0à
01>ü10E00E/X Ô0T3X0ì %# 4>à/^ l . 2,, \$1>è#T>ä 1~0È &€ /x ô/X*# *401 # \$0 h %1• 1 1
\$0 l 0ü (111) #ü0ì 1~1~ Ü 7\$>à#ü*# 01>ü <A*10ì &/^ h , 0Ü3Y/X •3H/È =ä#ü/X •3H
0E0à *!?À1 010ì ;=>ü <ô*10ü 81• 0ì ?Ý1 >à/^ l . &€ /x ô ,,1•/X*# %# 4 #
1 1 0à 10E ,?Ü>á1%01>ü <A*10È ,l1# %1• 6'#l# œ1 1 >ð/X 1 /< ,2^0ì 1# ,d>è
0ü l . €)X#T .ì P! ™6'#l 0Ü01'//È ;0È /t!t /<>"#48^0ü*à #%#/X L 2™0 >ä/u>è0ì
|•>è 0ü l .

>ý,t/< : 1#1 0X#410E*8/x"T10E3H 1 1 , <ô*1 , //?Ü#Ü8l P3

~*40à ^ (Acknowledgments)

#Ä1^ 3H•L *<.lL*Ü*¤ /° #T\$Ä0ì 2,,^>à,d >à ` .l& 3H ` ~*4# d#E P I . '1ù>ä 2,,0à 2 , }>è + 1 0È?¤# ?P!>à,d/< DGIST /X*¤ *¥*4>á0CE# %£ >à,t0ì ~*4 d#E P I . T 0ü8¤&|#ü >à `0à *4! 0Ä!ä 3H /° Ø >ü/`= P I . A l/< .x!t3P Ô, ,(X >à#ø 3 ø0T>è Ô, /@1¤ 1^0à *>,, a? >à,d >à ` .l& 3H# ,h"8>à h *4\$0>ñ P I .

*¥*4>á0CE,,1• a.Ð #V0È' l0ü >ð `>ü 2,,*ð,= P I . #Ä1^ >á1 0à Ä!ä .l^h1 >à 1^X 1*1 /<#8 3H L/È ^,t0ì ^1Ä2,,h >ä&Y5' Ø+ `` ~*40à #X.^0ì d#E P I . €#4 h \$Ä0ì /!1>à ,,1/X*¤ 0^0ý>ä 1ø/@ì >ü2,,h È>à*¥ Ø+ ` , 0-/%o , %*4 `` L ~*40à 1*4# d#E P I .

\$¼/O&|I AIC ODES a*e l0ü ^1- ,/=X 0,= P I . '1ù>ä ?•0ü1 /-è1 1^# %,!->ü2,,h 1!->ü 2^ ,A@0/È1 ?¤/X ~*40à 1*4# 1CE>ñ P I 0ü à0ì ;=>ü >á\$ÄX#T.l!P! >à 1 CE0Ä!ä *¤ /< C *<.l^/ >à 3H #V0ü %o,08 /P,= P I . ~>ä /x ô,l0à h h>ä &<\$10ü*ð à *¤%,?Ä %*4 `` L ~*4# d#E P I . 1*e **%,!ä*¤ €#4 h >á\$Ä **%,!ä*¤ %*4 `` *¤ >ü2,,*ð à + #V0È 1ø/@,, 1!-^ 9ø A 0ü /P,= P I . %o,0@1~0ü #V0È1!,,!x @L%,1*I@è0ü/È 2^@ô á Ô3H >ð ` >è + /N/P3H#T08#40à 2 0È & 1 ?¤%,0ü/X L ~*40à 1*4# 1CE>ñ P I €#4 h a,1 a ?à ?•, 1/x ?•, /%o2^ ?•, +¤09ü, 0X Ø ^%o0ü, >à/%øü, 0^%€ a@, 0È/%øü, A l }>à h 1 0 ð1 7ä ô Jakkid, Kriangsak, Prak ash # !ì!->ä /X•3H ,,0à \$0 h ' ` h#a l 1 *4l d#E P I . €#4 h 1^0à & 1 5^?CE0ü &Y1 0ü &Y08 1%€ a0X, \$>ä0ü /X L h#a l #X 0ì 1CE>à h,~,= P I .

/%o.Ð Ø@ # *´ , \$0 h ' l ` L ~*4 # d#E P I . #Ä1^ |1 \$1*4`0ü,h \$Ä*!e \$1*4` , h h >ä /,, *´ '\$1*4` , , L/È 1ø/@0ì.l 3H .00Ä*ð à ,*¥0ü ?•, /%o , ?•, L&Y0ü ?•, 14%,0ü?•, 713L0ü &Y60ü# !ì!->ä >CE!ä;(, 65 l' @ 0X l/X 3L,t0Ä!ä ~*4# d#E P I . 0ü l0à 2™&| , L# ;=>ü >à ``*¤ 1^0à *>0ì 0ü Ô/< 2,,*ð,= P I .

#P3H#Q0Ä!ä4! >à 08#4 ^1ù , &Y*I/X*¤ L >ü#Y + 1 # #f0ü>ü2,,d >è#Ä P, Ô1/N *4 ! 0ì 2,,d#ø %ce#,h.á0à &€0ü ,d .l& 3H /<#Ä P, €#4 h *4! >à a*e ,, /t1 7ä ð1 ?¤+ , 0ü l0à , L/È ?T,h0ü 1/P ,/X *¥*4>á0CE,,1•0ì #P\$¼#4>è 1/P,= P I . *4! >ñ P I . 7 &}>ñ P I .

Curriculum Vitae

Name: Joon Kyo Seo

Birth Date: 11/28/1983

Education

School	Location	Major	Dates	Degrees
Daegu Gyeongbuk Institute of Science and Technology (DGIST)	Daegu, Republic of Korea	Energy Systems Engineering	Mar. 2011 present	M.S.
Kyungpook National University	Daegu, Republic of Korea	Electrical Engineering	Mar. 2003 Feb. 2010	B.S.E.
University of Hawaii at Manoa	Honolulu, HI	Electrical Engineering	Aug. 2008 May 2009	International Exchange Student

Work Experience

LG Electronics Inc.

Research Engineer / AE Advanced Control Group, AE Control R&D Lab. Changwon, Republic of Korea

- Development of solar inverters
- Analysis of battery management system for LIB

Jan. 2010 | Jan. 2011

Journal Publications

1. **J. K. Seo**, A. Khetan, M. H. Seo, H. Kim and B. Han, " First-principles thermodynamic studies on the electrochemical stability of Pt nanoparticles in fuel cell applications", *submitted to the Journal of Power Sources*
2. M. H. Seo, S. M. Choi, **J. K. Seo**, S. H. Noh, W. B. Kim and B. Han, " The graphene-supported palladium and palladium-yttrium nanoparticles for the oxygen reduction and ethanol oxidation reactions: Experimental measurement and Computational validation", *Appl. Catal. B-Environ.* 129 (2013) 163-171 (IF = 5.625)

Patent Applications

1. K.-R. Park and **J. K. Seo**, "Photovoltaic power generation system" **Korean Patent, Application Number 10-2010-0136477**

International Conference Presentations

1. **J. K. Seo**, and B. Han, "First-Principles Approach on the Electrochemical Dissolution Processes of Pt Nanocatalysts" The 63rd Annual Meeting of the International Society of Electrochemistry, Prague, Czech Republic, (Aug. 19-24, 2012)

Awards and Honors

- National Scholarship (full tuition)
(Spring 2011 – Fall 2012, Daegu Gyeongbuk Institute of Science and Technology, Republic of Korea)
- National Science and Engineering Undergraduate Scholarship (full tuition)
(Fall 2003 – Spring 2005, and Fall 2008- Fall 2009, Korea Student Aid Foundation, Republic of Korea)
- Foreign Exchange Student Scholarship
(Fall 2008 – Spring 2009, Kyungpook National University, Republic of Korea)
- Nuri (New University for Regional Innovation) Scholarship
(Fall 2008, Ministry of Education and Human Resources Development, Republic of Korea)
- Nuri learnfare scholarship
(Fall 2008, Ministry of Education and Human Resources Development, Republic of Korea)

Teaching

- Teaching assistant for Daegu Il Science High School – Quantum Computational Design of High Functional Materials for Renewable Energy Systems May 2012 – present

